REPORT DOCUMENTATION PAGE

Form Approved
OMB No. 0704-01-0188

PLEASE DO NOT RETURN YOUR FORM TO THE ABOVE ADDRESS.

1. REPORT DATE *(DD-MM-YYYY)*	2. REPORT TYPE	3. DATES COVERED *(From - To)*
21-03-2006	REPRINT	

4. TITLE AND SUBTITLE
Ion chemistry of NOO^+

5a. CONTRACT NUMBER

5b. GRANT NUMBER

5c. PROGRAM ELEMENT NUMBER
61102F

6. AUTHORS
A.J. Midey*, A.I. Fernandez**, A.A. Viggiano, P. Zhang#, and K. Morokuma##

5d. PROJECT NUMBER
2303

5e. TASK NUMBER
BM

5f. WORK UNIT NUMBER
A1

7. PERFORMING ORGANIZATION NAME(S) AND ADDRESS(ES)
Air Force Research Laboratory /VSBXT
29 Randolph Road
Hanscom AFB, MA 01731-3010

8. PERFORMING ORGANIZATION REPORT NUMBER
AFRL-VS-HA-TR-2006-1043

9. SPONSORING/MONITORING AGENCY NAME(S) AND ADDRESS(ES)

10. SPONSOR/MONITOR'S ACRONYM(S)
AFRL/VSBXT

11. SPONSOR/MONITOR'S REPORT NUMBER(S)

12. DISTRIBUTION/AVAILABILITY STATEMENT
Approved for public release; distribution unlimited.

13. SUPPLEMENTARY NOTES
Reprinted from J. Chem. Phys., V. 124, 114313 (2006) doi:10.1063/1.2177257 * Boston College, Chestnut Hill, MA 02467 **Argonne Nat'l Lab., Argonne, IL ##Emory Univ., Atlanta, GA 30322 #Present address: Harvard-Smithsonian Ctr., Cambridge, MA

14. ABSTRACT

The kinetics for the reactions of NOO^+ ions with neutral molecules having ionization potentials (IPs) from 9.27 to 15.58 eV was measured in aselected ion flow tube at 298 K. The NOO^+ ions are produced from the reaction of $N_3^+ + O_2$, and have been reacted with the following: NO, C_6F_6, CS_2, CF_3I, C_3F_6, OCS, C_2H_6, Xe, SO_3, O_3, N_2O, CO_2, Kr, CO, D_2, and N_2. Numerous types of reactions were observed with the various neutral reagents, including production of NO^+ (which may involve loss of an O from the ion or addition of O to the neutral reactant, although the two channels could not be distinguished here), charge transfer, isomerization of NOO+ to ONO+, and hydride abstraction. High level theoretical calculations of the structures and energetics of the various isomers, electronic states, and transition states of NOO and NOO^+ were performed to better understand the observed reactivity. All neutral species with an IP $\leq$11.18 eV were observed to react with NOO+ in part by charge transfer. Detailed calculations showed that the recommended adiabatic and vertical IPs of NOO are 10.4 and 11.7 eV, respectively, at the MRCISD(Q)/AVQZ level of theory. The observed experimental limit for charge transfer of 11.18 eV agreed well with the energetics of the final products obtained from theory if dissociation of the neutral metastable product occurred, i.e., the products were $X^+ + [O(^3P) + NO(^2\Pi)]$ formed via dissociation of metastable NOO. Charge exchange with neutral reagent X would, therefore, be exothermic if $IP(X) < [IP^{ad}(NOO) - E_{(O+NO)-NOO}] = \sim 11.1$ eV, where $IP^{ad}(NOO)$ is the adiabatic IP. The potential energy surface for the reaction of NOO+ with C2H6 was also calculated, indicating that two pathways for formation of $HNO_2 + C_2H_5^+$ exist.

15. SUBJECT TERMS
Rate constant
Nitrogen dioxide cation
ion chemistry
ionization potential

16. SECURITY CLASSIFICATION OF:			17. LIMITATION OF ABSTRACT	18. NUMBER OF PAGES	19a. NAME OF RESPONSIBLE PERSON
a. REPORT	b. ABSTRACT	c. THIS PAGE			A. A. Viggiano
UNCL	UNCL	UNCL	UNL		19B. TELEPHONE NUMBER *(Include area code)* (781) 377-4028

Ion chemistry of NOO^+

A. J. Midey,[a] A. I. Fernandez,[b] and A. A. Viggiano[c),d]
Air Force Research Laboratory, Space Vehicles Directorate, Hanscom Air Force Base, Massachusetts 01731-3010

P. Zhang[e] and K. Morokuma[c),f]
Cherry L. Emerson Center for Scientific Computation, Emory University, Atlanta, Georgia 30322 and Department of Chemistry, Emory University, Atlanta, GA 30322

(Received 19 December 2005; accepted 24 January 2006; published online 21 March 2006)

The kinetics for the reactions of NOO^+ ions with neutral molecules having ionization potentials (IPs) from 9.27 to 15.58 eV was measured in a selected ion flow tube at 298 K. The NOO^+ ions are produced from the reaction of $N_3^+ + O_2$ and have been reacted with the following: NO, C_6F_6, CS_2, CF_3I, C_3F_6, OCS, C_2H_6, Xe, SO_2, O_3, N_2O, CO_2, Kr, CO, D_2, and N_2. Numerous types of reactions were observed with the various neutral reagents, including production of NO^+ (which may involve loss of an O from the ion or addition of O to the neutral reactant, although the two channels could not be distinguished here), charge transfer, isomerization of NOO^+ to ONO^+, and hydride abstraction. High level theoretical calculations of the structures and energetics of the various isomers, electronic states, and transition states of NOO and NOO^+ were performed to better understand the observed reactivity. All neutral species with an IP $\leqslant$ 11.18 eV were observed to react with NOO^+ in part by charge transfer. Detailed calculations showed that the recommended adiabatic and vertical IPs of NOO are 10.4 and 11.7 eV, respectively, at the MRCISD(Q)/AVQZ level of theory. The observed experimental limit for charge transfer of 11.18 eV agreed well with the energetics of the final products obtained from theory if dissociation of the neutral metastable product occurred, i.e., the products were $X^+ + [O(^3P) + NO(^2\Pi)]$, where $[O(^3P) + NO(^2\Pi)]$ formed via dissociation of metastable NOO. Charge exchange with neutral reagent X would, therefore, be exothermic if $IP(X) < [IP^{ad}(NOO) - \Delta E_{(O+NO)-NOO}] = \sim 11.1$ eV, where $IP^{ad}(NOO)$ is the adiabatic IP. The potential energy surface for the reaction of NOO^+ with C_2H_6 was also calculated, indicating that two pathways for formation of $HNO_2 + C_2H_5^+$ exist. © *2006 American Institute of Physics.* [DOI: 10.1063/1.2177257]

I. INTRODUCTION

The reaction of N_3^+ with O_2 proceeds by two channels,

$$N_3^+ + O_2 \rightarrow NO^+ + (N_2O) \quad (1a)$$

$$\rightarrow NO_2^+ + N_2, \quad (1b)$$

where N_2O is shown in parentheses because several different neutral fragments can be formed exothermically. Several studies of reaction (1) have been performed, a number of which have indicated that the NO_2^+ product has the isomeric form NOO^+.[1–7] Our groups have recently studied this reaction over an extended temperature range showing that channel (1b) diminished substantially with increasing temperature from 120 to 1400 K.[6] In that study, it was conclusively shown that the NO_2^+ isomer formed was not the ONO^+ form made by ionizing ONO.

While reaction (1) has been studied extensively, little research has been performed to elucidate the ion chemistry of NOO^+. Matusoka *et al.*[5] found in a time resolved atmospheric pressure ionization (TRAPI) instrument that the NO_2^+ ions formed in reaction (1) were lost in collisions with N_2. The experiments showed that the NOO^+ reaction with N_2 formed NO^+ (assumed to be from thermal dissociation of NOO^+) and that the reaction had an activation energy associated with it.[7] On the other hand, Hiraoka[4] showed that these ions do not react in a high-pressure mass spectrometer (HPMS). The latter results were consistent with *ab initio* calculations of the successive binding energies of N_2 ligands in $NO_2^+(N_2)_n$ clusters containing ONO^+.[8] In addition, the calculations further indicated that NOO^+ was not stable. In the TRAPI experiments, it was further shown that the NO_2^+ produced in reaction (1) reacted with C_2H_6 to form $C_2H_5^+$, whereas ONO^+ ions did not react with C_2H_6, again indicating that the NOO^+ isomer is formed in reaction (1).[7]

All of the above studies were made in complicated mixtures of gases involving multiple steps in the observed reactions. However, in our recent study of reaction (1) in a selected ion flow tube (SIFT),[6] we could better control the chemistry to produce NOO^+ than in the previous experiments. N_3^+ ions were injected into a pure He buffer where O_2

[a)]Also at the Institute for Scientific Research, Boston College, Chestnut Hill, MA. Electronic mail: anthony.midey@hanscom.af.mil
[b)]Present address: Argonne National Laboratory, Argonne, IL.
[c)]Authors to whom correspondence should be addressed.
[d)]Electronic mail: albert.viggiano@hanscom.af.mil
[e)]Present address: ITAMP Harvard-Smithsonian Center for Astrophysics, Cambridge, MA.
[f)]Electronic mail: morokuma@emory.edu

was added in substantial quantity through an upstream inlet to produce NO^+ and NO_2^+, neither of which reacted with O_2. After reaction (1) was driven to completion, Xe was added downstream to distinguish between the two NO_2^+ isomers. We found that the NO_2^+ formed in reaction (1) reacted with Xe and that ONO^+ produced from ONO did not. This conclusively showed that N_3^+ reacts with O_2 to form NO_2^+ in the NOO^+ form.[6]

In the present study, the ion chemistry of NOO^+ is examined in more detail in a SIFT at 298 K, where reaction (1) was used to create NOO^+ in the flow tube. The following molecules were used as neutral reagents, listed in order of increasing ionization potential (IP): NO, C_6F_6, CS_2, CF_3I, C_3F_6, OCS, C_2H_6, Xe, SO_2, O_3, N_2O, CO_2, Kr, CO, D_2, and N_2. Using molecules with IP values ranging from 9.27 to 15.58 eV brackets the IP for NOO and gives insight into the reactivity of NOO^+. Numerous types of reactions are observed with the various neutral reagents, including production of NO^+ (which may involve loss of an O or addition of O to the reactant neutral, although the two channels could not be distinguished here), charge transfer, isomerization of NOO^+ to ONO^+, and hydride abstraction. Based on the diversity of the observed chemistry, the measurements have been complemented by high level theoretical calculations of the structures and energetics of the various isomers, electronic states, and transition states of NOO and NOO^+. In addition, the potential energy surface for the reaction of NOO^+ with C_2H_6 has also been calculated.

II. EXPERIMENTAL METHOD

The measurements were made in a selected ion flow tube (SIFT) that has been thoroughly described previously.[9,10] Briefly, N_3^+ ions were generated from N_2 in an effusive source in a high-pressure source region. Two mechanisms for N_3^+ production were operative: three-body association of N^+ with N_2 and Penning ionization of N_2, the latter of which is shown in Eq. (2),

$$N_2^* + N_2 \rightarrow N_3^+ + N. \quad (2)$$

The N_3^+ ions were mass selected and injected into the flow tube through a Venturi inlet, resulting in a small amount of N^+ from dissociation upon injection (<2%). Helium buffer gas (AGA, 99.995%) carried the ions downstream, where O_2 (Mass. Oxygen, 99.999%) was added 82 cm from the sampling orifice. The O_2 converted the N_3^+ ions into NO^+ and NOO^+ through reaction (1). Sufficient O_2 was added such that the reaction was driven to completion before either of the two reactant inlets, which were located at 36 and 52 cm from the sampling orifice. The reactant gas was added through one of these inlets and the kinetics was mostly studied in the normal fashion, since neither NO^+ nor O_2 generally reacted with the ionic products or neutral reagents studied. The average relative error in the rate constants is ±15% and the absolute error is ±25%.[10] All of the neutral reagents were used as obtained from the manufacturer.

A few complications did arise. In the reactions of NOO^+ with SO_2 and CS_2 some ONO^+ was produced through isomerization. This ion obviously has the same mass as

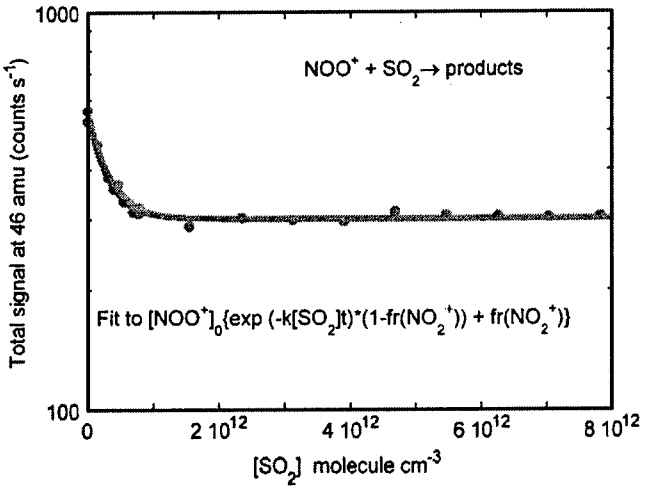

FIG. 1. Plot of total ion signal at m/z=46 amu vs concentration of SO_2 for the reaction of $NOO^+ + SO_2$ measured in a selected ion flow tube (SIFT) at 298 K.

NOO^+ (m/z=46), resulting in curvature in the rate constant plots. An example for the SO_2 reaction is shown in Fig. 1. Since ONO^+ did not react with SO_2, the 46 amu signal leveled off at higher SO_2 flows when all of the NOO^+ was reacted away. Thus, the ratio of the NO_2^+ signal in the flat portion of the curve to that portion with no SO_2 added gave the branching fraction for ONO^+ production. To obtain the rate constant k, the NO_2^+ signal in Fig. 1 observed after reaction time t was fitted to Eq. (3),

$$[46\text{ amu}] = [46\text{ amu}]_0\{\exp^{(-k[SO_2]t)}(1 - \%\,ONO^+/100) + (\%ONO^+/100)\}, \quad (3)$$

which also yields the branching into the two product channels. Another complication arose in the Xe reaction, where a small amount of the observed Xe^+ signal was attributed to the slow reaction of O_2^+ (formed from N^+ present in the flow tube reacting with O_2) with Xe. However, the contribution of the O_2^+ reaction to the Xe^+ signal can be easily subtracted. Lastly, the NO^+ formed in a number of the NOO^+ reactions had a background contribution due to reaction (1). Consequently, the NO^+ formed in the reactions with NOO^+ is simply the difference between the amount of NO^+ observed with and without the reactant neutral added.

III. CALCULATION METHOD

As will be discussed later, the ionization potential (IP) of NOO is very crucial to understanding the charge transfer mechanism and one of the main goals of the present study is to determine its value. Therefore, we calculated the IP at various levels of theory. More specifically, the geometries of ground state $NOO(^2A')$ and $NOO^+(^1\Sigma^+)$ were optimized at the CASPT2 and ROHF-UCCSD(T) levels of theory along with Dunning's correlation consistent polarized valence quadruple-zeta basis set augmented with diffuse functions (aug-cc-pVQZ), denoted as AVQZ.[11] Here, CASPT2 refers to internally contracted second-order multireference perturbation theory.[12] In the CASPT2 calculation, all the orbitals except the 1*s* were involved in the correlation treatment and the

TABLE I. Kinetics of the reactions of NOO^+ with neutral molecule X at 298 K. The Su-Chesnavich collision rate constant k_c (Refs. 28 and 29) is given in brackets.

X IP (eV)	k [k_c][a] ($cm^3\ s^{-1}$)	Products	Branching ratio	$\Delta H_{rxn}^{298\ K}$ ($kJ\ mol^{-1}$)	X IP (eV)	k [k_c][a] ($cm^3\ s^{-1}$)	Products	Branching ratio	$\Delta H_{rxn}^{298\ K}$ ($kJ\ mol^{-1}$)
NO	8.9 [7.6]	$NO^+ + NOO$	>0.98	−118.7[b]	C_2H_6	10 [12]	$C_2H_5^+ + HNO_2$	1.00	−499
9.27		$O_2^+ + N_2O$	<0.02	−251	11.50				
C_6F_6	8.2 [12]	$C_6F_6^+ + NOO$	0.91	−48	Xe	5.7 [8.1]	$NO^+ + XeO$	0.97	−350[c]
9.90		$NO^+ + C_6F_6 + O$	0.09	−211	12.13		$XeO^+ + NO$	0.03	−108[c]
CS_2	15 [13]	$NO^+ + CS_2 + O$	0.17	−174	SO_2	10 [18]	$NO^+ + (SO_3)$	0.55	−174
10.07		$SO^+ + CS + NO$	0.14	−155	12.35		$ONO^+ + SO_2$	0.45	−434
		$ONS^+ + (OCS)$	0.03	−686[d]					
		$SO_2^+ + (CN + S)$	0.11	79[e]	O_3	5.1 [10]	$NO^+ + 2O_2$	0.98	−566
		$CS_2^+ + NOO$	0.41	−42	12.53		$O_2^+ + NO_3$	0.02	−314
		$ONO^+ + CS_2$	0.14	−434					
					N_2O	0.15 [9.0]	$NO^+ + N_2 + O_2$	1.00	−505
CF_3I	11 [14]	$NO^+ + CF_3I + O$	0.55	−174	12.89		$NO^+ + N_2O + O$		−174
10.28		$CF_3^+ + ONO + I$	0.18	−280					
		$OI^+ + CF_3 + NO$	0.01	−198[f]	CO_2	<0.002	No reaction		
		$FI^+ + CF_2 + ONO$	0.12	−38	13.78				
		$CF_3I^+ + NOO$	0.14	−27					
					Kr	<0.03	No reaction		
C_3F_6	9.8 [14]	$NO^+ + C_3F_6 + O$	0.73	−174	14.00				
10.60		$C_2F_4N^+ + CO_2 + F_2$	0.10	55[g]					
		$C_3F_5^+ + (FNO_2)$	0.04	−109[h]	CO	7.9 [8.0]	$NO^+ + CO + O$	0.95	−174
		$C_3F_6^+ + NOO$	0.13	10[i]	14.01		$O_2^+ + NCO$	0.05	−1
OCS	8.9 [13]	$OCS^+ + NOO$	0.18	61	D_2	<0.02	No reaction		
11.18		$SO^+ + CO + NO$	0.23	−289	15.47				
		$NO^+ + CO + SO$	0.59	−391					
					N_2	<0.008	No reaction		
					15.58				

[a]All rate constants shown are $\times 10^{-10}$.
[b]Charge transfer reaction enthalpies calculated assuming neutral NOO for all cases.
[c]Taken from Ref. 6.
[d]ΔH_f^0(298 K) ONS^+ from G3(B3LYP) calculation.
[e]ΔH_f^0(298 K) SO_2^+ from ΔH_f^0 SO_2 and IP of SO_2.
[f]ΔH_f^0(298 K) OI^+ from Hassanzadeh and Irikura (Ref. 31).
[g]ΔH_f^0(298 K) $C_2F_4N^+$ from G3(B3LYP) calculation.
[h]ΔH_f^0(298 K) $C_3F_5^+$ upper limit from Jarvis *et al.* (Ref. 32).
[i]ΔH_f^0(298 K) $C_3F_6^+$ from ΔH_f^0 C_3F_6 and IP of C_3F_6.

reference wave function was obtained from the corresponding full valence state specific complete active space self-consistent field[13,14] (CASSCF) calculation, which included 17 and 16 electrons distributed over 12 orbitals for the neutral and ionic species, respectively. ROHF-UCCSD(T) refers to the spin unrestricted open shell coupled-cluster singles and doubles[15] augmented by triple excitation noniteratively.[16] In this scheme, the standard RHF-CCSD(T) is used for the closed shell systems. For the open shell system, the ROHF calculation was performed first, from which unrestricted molecular orbitals (MOs) were created, followed by UCCSD calculations. To further refine the energetics, a single-point multireference configuration interaction MRCISD(Q) calculation was carried out on top of the CASPT2 optimized geometry using the same AVQZ basis set. MRCISD(Q) refers to the internally contracted multireference configuration interaction including both single and double excitations[17,18] (MRCISD) plus the multireference version of the Davidson correction (Q).[19] Similar to the CASPT2 calculation, only the 1s orbitals were excluded in the correlation treatment and the same full valence state specific CASSCF wave functions also served as the references. All the calculations were performed using the MOLPRO 2002.6 quantum chemistry program package.[20]

IV. RESULTS AND DISCUSSION

A. Experimental results

Rate constants and product branching ratios for the NOO^+ reactions studied at 298 K are listed in Table I. The neutral reagents are listed in order of increasing ionization potential (IP). The heats of reaction at 298 K shown in Table I have been calculated using the standard heats of formation available in the NIST Chemistry Webbook,[21] except where noted. For the less common species $C_2F_4N^+$ and ONS^+, no

TABLE II. Optimized NOO and NOO^+ geometries (bond lengths R in Å and bond angles A in degrees) at different levels of theory. In all the multireference methods, full valence CASSCF space including 16 e^- (for NOO^+) or 17 e^- (for NOO) in 12 orbitals was used in the correlation calculation.

	$NOO(^2A')$			$NOO^+(^1\Sigma^+)$		
	R_{N-O}	R_{O-O}	A_{N-O-O}	R_{N-O}	R_{O-O}	A_{N-O-O}
CASSCF/AVTZ	1.2230	1.3709	120.3	1.1387	1.2321	180.0
CASPT2/AVQZ	1.2315	1.3482	122.6	1.1501	1.2289	180.0
RHF-UCCSD(T)/AVQZ	1.2128	1.3451	122.2	1.1379	1.2288	180.0
MRCISD(Q)/cc-pVTZ[a]	···	···	···	1.1459	1.2334	180.0

[a]Results are taken from Ref. 6.

literature values for the heats of formation were found. Therefore, the standard heats of formation at 298 K for these species were calculated using GAUSSIAN 03 for optimized geometries.[22] Both ONS and ONS^+ were observed experimentally by Andrews *et al.* using infrared (IR) spectroscopy and they were shown to have bent and linear structures, respectively, as verified by density functional theory (DFT) calculations at the B3LYP level.[23] Consequently, G3(B3LYP) theory[24] was used to calculate the heat of formation of ONS^+, yielding geometries for ONS and ONS^+ in good agreement with the previous calculations.[23] Analogous G3(B3LYP) calculations were done for C_2F_4N and $C_2F_4N^+$, the latter of which had been observed in trace amounts in the mass spectra from the analysis of perfluorocarbon compounds.[25–27] The minimum energy isomer of $C_2F_4N^+$ was located by first performing optimizations of 11 possible isomers of the neutral and the cation at the B3LYP/6-311++G(3*df*,2*p*)||B3LYP/6-31G(*d*) level. The wave function stability of all species needed to calculate the thermochemistry was verified as well. The heats of formation at 298 K obtained from these calculations are 976 ± 5 kJ mol^{-1} for ONS^+ and 185 ± 5 kJ mol^{-1} for $C_2F_4N^+$.

Most of the NOO^+ reactions occurred with a rate constant k at or near the Su-Chesnavich collision rate constant limit[28,29] k_c, i.e., $k/k_c > 0.5$ or 50% efficient. CO_2, Kr, D_2, and N_2 were found to be unreactive. N_2O was the only species that reacted slowly, with a rate constant around 1.7% of the collisional value, k_c. For the species with the lowest ionization potentials (NO and C_6F_6), the reaction proceeded predominantly via nondissociative charge transfer (>91% of products). For species with ionization potentials between 10.07 and 11.18 eV, charge transfer was still important (18%–41% of the products). For species with IP $\geq$ 11.5 eV, no charge transfer occurred. This observation implies that the IP of NOO is <11.5 eV. The calculations discussed below address this issue in more detail.

Production of NO^+ ions was found in the reactions of NOO^+ with NO, C_6F_6, CS_2, CF_3I, C_3F_6, OCS, Xe, O_3, N_2O, and CO. It was the predominant reaction channel for all species with IP $\geq$ 10.28 eV, except for C_2H_6, where no NO^+ was formed. Dissociation of NOO^+ into NO^+ plus O is exothermic, but a substantial barrier to unimolecular dissociation of NOO^+ exists.[6] However, in the course of an ion-molecule reaction, the barrier might disappear and the NO^+ product might be the result of either O atom transfer or simple dissociation induced by the proximity of the reactant neutral. Our experiment could not differentiate between the two possibilities.

Several of the reactions were quite complicated, resulting in three to six different product ions. Several unusual product species were observed, including ONS^+ (with CS_2), FI^+ and IO^+ (with CF_3I), $C_2F_4N^+$ (with C_3F_6), and XeO^+ (with Xe). The reactions of CS_2 and SO_2 caused isomerization of NOO^+ to ONO^+ in 14% and 45% of the reactions, respectively.

B. Ionization potential calculation

The optimized equilibrium geometries for NOO and NOO^+ are given in Table II and the calculated vertical and adiabatic IPs are collected in Table III. In general, the geometries from all of the methods used here agreed well with each other. The most significant difference was the N–O bond length. The multireference based correlated method yielded a longer bond length (~0.012 Å). The structure of NOO^+ had been investigated in our previous study at the MRCISD(Q) level of theory with the valence triple-zeta basis set (cc-pVTZ).[6] The optimized N–O distance was 1.146 Å, which lies in between the results of the CASPT2 and ROHF-UCCSD(T) calculations.

In contrast, the calculated IP values showed relatively large differences amongst the different theoretical methods, especially for the adiabatic IP. The general trend was that the MRCISD(Q) calculations predicted smaller values than the other two methods. The difference between the MRCISD(Q) and CASPT2 results was only ~0.1 eV. However, the most

TABLE III. Adiabatic and vertical ionization potentials (IPs) of $NOO(^2A')$ calculated at different levels of theory. In all the multireference methods, full valence CASSCF space including 16 e^- (for NOO^+) or 17 e^- (for NOO) in 12 orbitals was used in the correlation calculation.

	Vertical IP (eV)		Adiabatic IP (eV)	
	w/ZPE[a]	w/o ZPE	w/ZPE	w/o ZPE
MRCISD/AVQZ//CASPT2/AVQZ	11.69	11.75	10.44	10.35
CASPT2/AVQZ	11.75	11.81	10.53	10.44
ROHF-UCCSD(T)/AVQZ	11.97	12.05	11.46	11.37

[a]ZPE was only calculated at CASSCF/aug-cc-pVTZ level of theory based on the same CASSCF method optimized geometry. As for the vertical IP, projected frequency calculation was carried out also at the CASSCF level to obtain the ZPE value.

significant discrepancy was for the adiabatic IP obtained from the ROHF-UCCSD(T) calculation, which was ~1.0 eV higher than the MRCISD(Q) results. In our previous investigation of NOO^+, consistent results amongst the coupled-cluster, CASPT2, and MRCISD(Q) methods were obtained for the O–O bond cleavage process.[6] Therefore, the difference was likely from the description for the neutral open shell NOO species. The T_1 value[30] of 0.05 in the UCCSD(T) calculation of NOO indicates the extensively multireference nature of this species, which most likely caused the adiabatic IP to be overestimated. Therefore, the suggested values for adiabatic and vertical IPs of NOO are 10.44 (10.35) and 11.69(11.75) eV, respectively, from the MRCISD(Q) calculations, where the values in parentheses do not include the zero-point energy (ZPE) correction. At this level of calculation, the errors are expected to be around 0.1 eV.

These results provide a qualitative interpretation for the IP dependence observed in the experimental charge transfer branching ratios. Charge transfer is essentially nonadiabatic. Thus, the multireference methods are best suited to study this process. However, in the present system, it is too computationally expensive to perform comprehensive investigations at this level of theory. Consequently, a potential energy surface (PES) scan was performed to qualitatively explain the trends observed in the experiments.

As seen in Table I, the fraction of reaction occurring by charge transfer decreased with increasing IP and shut off at IPs over 11.18 eV. Using the reaction of NOO^+ with NO as an example, we scanned the PESs involved at the same MRCISD(Q) level of theory. The scan was carried out with the NOO and NO species at infinite separation. Two states corresponding to the $NOO+NO^+$ and NOO^++NO asymptotes, respectively, were scanned along the NOO bending coordinate with all other degrees of freedom fixed at the equilibrium geometries of $NOO^+(^1\Sigma^+)$ and $NO(^2\Pi)$. The results are shown in Fig. 2. Clearly, the two asymptotes cross in the vicinity of the linear $NOO^+(^1\Sigma^+)$ minimum region. Upon bending, these two states will cross at the minimum of the seam of crossing (MSX) marked in Fig. 2. The energy of this MSX is about ~0.15 eV relative to the $NOO^+(^1\Sigma^+)$ $+NO(^2\Pi)$ asymptote, which is below the ZPE level (0.23 eV) of $NOO^+(^1\Sigma^+)$. During the approach of the NO species, NOO^+ and NO might form a weak van der Waals complex with little change in the geometries of the individual species. On the contrary, this region corresponds to a high-energy regime of the PES originating from NOO $+NO^+$ because of the nonlinear minimum of the NOO species. Thus, this crossing point will be sampled every time the NOO^+ molecule vibrates. At infinite separation, however, the nonadiabatic coupling element between these two manifolds is zero. As the two species approach, the degeneracy of these states will be lifted and a nonvanishing coupling element between states with the same spin symmetry will grow, resulting in charge exchange. Besides the crossing on the bending coordinate, crossing on other coordinates (N–O and O–O stretchings) should provide little contribution because of the higher energy requirements as shown in the previous MRCISD(Q) study of NOO^+.[6]

It should be noted that the IP of NO is 9.27 eV, which is lower than the adiabatic IP of NOO. Thus, the crossing between these two PESs must be higher in energy than the asymptote of NOO^++NO, as schematically shown in Fig. 3. The charge transfer minimum seam of crossing (CT-MSX) is located in the vicinity of the NOO^++NO potential well, represented more generally as NOO^++X in Fig. 3. As the IP value for neutral molecule X increases, the second curve representing the PES for $NOO+X^+$ (curve 2) will begin to shift higher in energy, as illustrated by the dashed line. As a consequence, a charge transfer barrier will arise and charge transfer should cease to be important at neutral IP values above the adiabatic IP of NOO. However, this mechanism seems to contradict the experimental results that showed charge transfer for several species with adiabatic IPs above that of NOO.

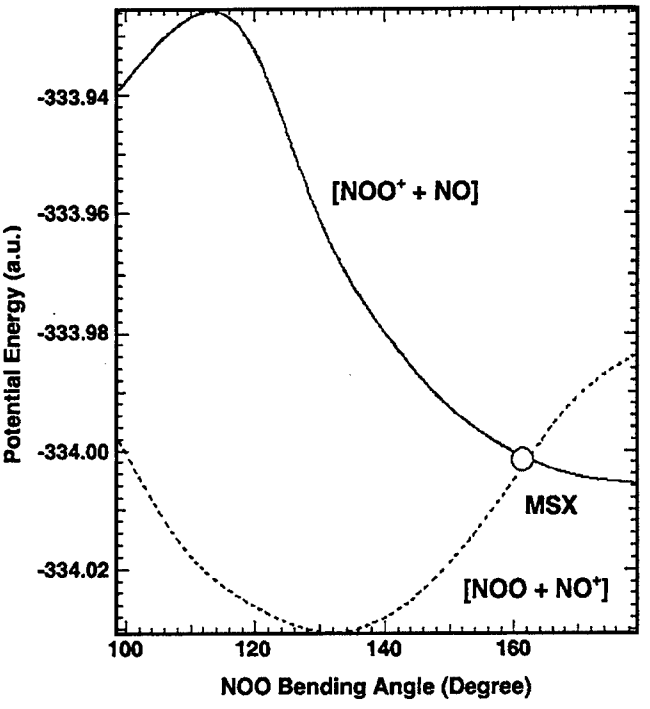

FIG. 2. Potential energy vs NOO bending angle for the NOO^++NO reaction system at the MRCISD(Q) level of theory (see text for details).

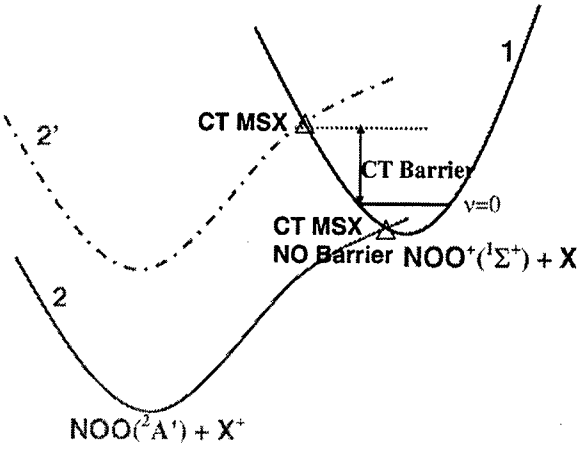

FIG. 3. Schematic potential energy surfaces for the reaction of NOO^++X, labeled as 1. Solid line curve labeled as 2 is for $NOO+NO^+$ and the dashed curve labeled as 2′ is for X with a much higher ionization potential (IP).

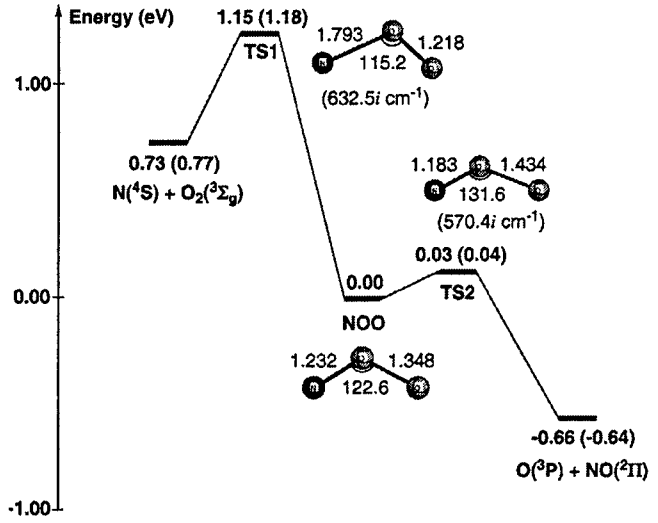

FIG. 4. ZPE corrected potential energy surface for the dissociation of NOO at MRCISD(Q)/AVQZ‖CASPT2/AVQZ level (energetics in parentheses are not ZPE corrected). Numbers on the structures refer to the bond length (Å) and bond angles (degree). The imaginary frequencies at TSs are given in the parentheses.

This observation subsequently implies that another mechanism must be occurring, at least for molecules with IPs above, or even near, the adiabatic IP of NOO. The mechanism outlined in Fig. 3 assumed that NOO was formed. However, NOO is metastable, as shown in the potential energy diagram in Fig. 4. There are two dissociation processes associated with the ground state NOO, the N–O and O–O bonding fissions. Two corresponding transition states, TS1 and TS2, were located at the CASPT2/AVQZ level of theory as shown in Fig. 4 and confirmed by the frequency and intrinsic reaction coordinate (IRC) calculations performed at the CASSCF/AVTZ level. The N–O bond breaking reaction, which leads to the $N(^4S)+O_2(^3\Sigma_g)$ products, must cross over a high barrier of 1.15 eV (TS1) at the single-point MRCISD(Q)/AVQZ level of theory. In contrast, a small barrier of 0.03 eV (TS2) will easily result in the O–O breaking and form the $O(^3P)+NO(^2\Pi)$ product with the exothermicity of $-\Delta E_{(O+NO)-NOO}=0.66$ eV at the same MRCISD(Q)/AVQZ level. Clearly, the NOO species produced via the CT process will almost exclusively dissociate into the $O(^3P)+NO(^2\Pi)$ products due to the extremely small barrier and the large internal energy gained from the CT reaction. As illustrated in Eq. (4), charge transfer will be exothermic for neutral reagents X with an $IP<(IP^{ad}(NOO)-\Delta E_{(O+NO)-NOO})=10.44+0.66=11.10$ eV, where $IP^{ad}(NOO)$ is the adiabatic IP,

$$NOO^+ + e^- \rightarrow NOO, \quad \Delta H = -IP^{ad}(NOO) = -10.44 \text{ eV}, \tag{4a}$$

$$X \rightarrow X^+ + e^-, \quad \Delta H = IP_x, \tag{4b}$$

$$NOO \rightarrow O(^3P) + NO(^2\Pi), \quad \Delta H = \Delta E_{(O+NO)-NOO} = -0.66 \text{ eV}, \tag{4c}$$

$$NOO^+ + X \rightarrow X^+ + O(^3P) + NO(^2\Pi), \quad \Delta H_{tot} = IP_x - IP^{ad}(NOO) + \Delta E_{(O+NO)-NOO}. \tag{4d}$$

Within the uncertainty, the energetics agrees well with the experimental limit of 11.2 eV. In essence, the overall mechanism is dissociative charge transfer. Typically, dissociative charge transfer is only experimentally observed if the ionic product dissociates, which is easily detected. However, the present calculations indicate that for the species with the highest IPs where charge transfer occurred, the neutral fragment dissociation must also have occurred and might also have occurred in all of the other charge transfer reactions.

C. $NOO^+ + C_2H_6$ potential energy surface

While detailed calculations for all of the reactions in Table I are not practical, we have performed additional calculations on the hydride abstraction reaction of NOO^+ with ethane (C_2H_6). The optimized reaction intermediates, transition states, and the various possible products are shown in Fig. 5 along with the corresponding potential energy profile. Due to the size of the system, the calculations were only carried out using density functional theory at the B3LYP/aug-cc-pVTZ level of theory. The product HNO_2 structures in Fig. 5 are labeled with the symmetry of the species in the name and are numbered from the highest energy product starting as number 1 to the lowest energy product of a given symmetry.

Basically, three possible reaction channels were identified for the reaction of NOO^+ with C_2H_6. The two lowest energy channels pass through transition states TS1 and TS2, which are below the energy of the reactants. Both TSs lead to $C_2H_5^+$ with the corresponding $HNO_2\_C_s\_1$ neutral product, having an exothermicity of -175.4 kJ mol^{-1}. The energies of these two TSs are almost the same, separated by <2 kJ mol^{-1}. Therefore, they might contribute similarly to the reactivity, although entropic effects would also play a role. The fact that these transition states have lower energies than the reactants suggests that van der Waals complexes must exist. These complexes are labeled as INT1 and INT2 in Fig. 5. However, van der Waals complexes were not located at the current level of computation. This must be related to the inability of the density functional method in describing the dispersion interaction, but it was not very important for understanding the overall reactivity. The third possible reaction channel would proceed through the higher energy TS3 to produce an isomer of HNO_2 as the neutral fragment that features a significantly stretched O–O bond, given as $HNO_2\_C_s\_4$ in Fig. 5. Clearly, the major difference between the third channel and the first two channels is that the terminal O atom of NOO^+ will abstract the H atom from C_2H_6 along the highest energy pathway, while the N atom of NOO^+ will abstract the H atom along the two lower energy pathways. An activation energy of 14.6 kJ mol^{-1} would be required to surmount TS3, which makes this pathway less important at low energy or temperature. Nevertheless, reac-

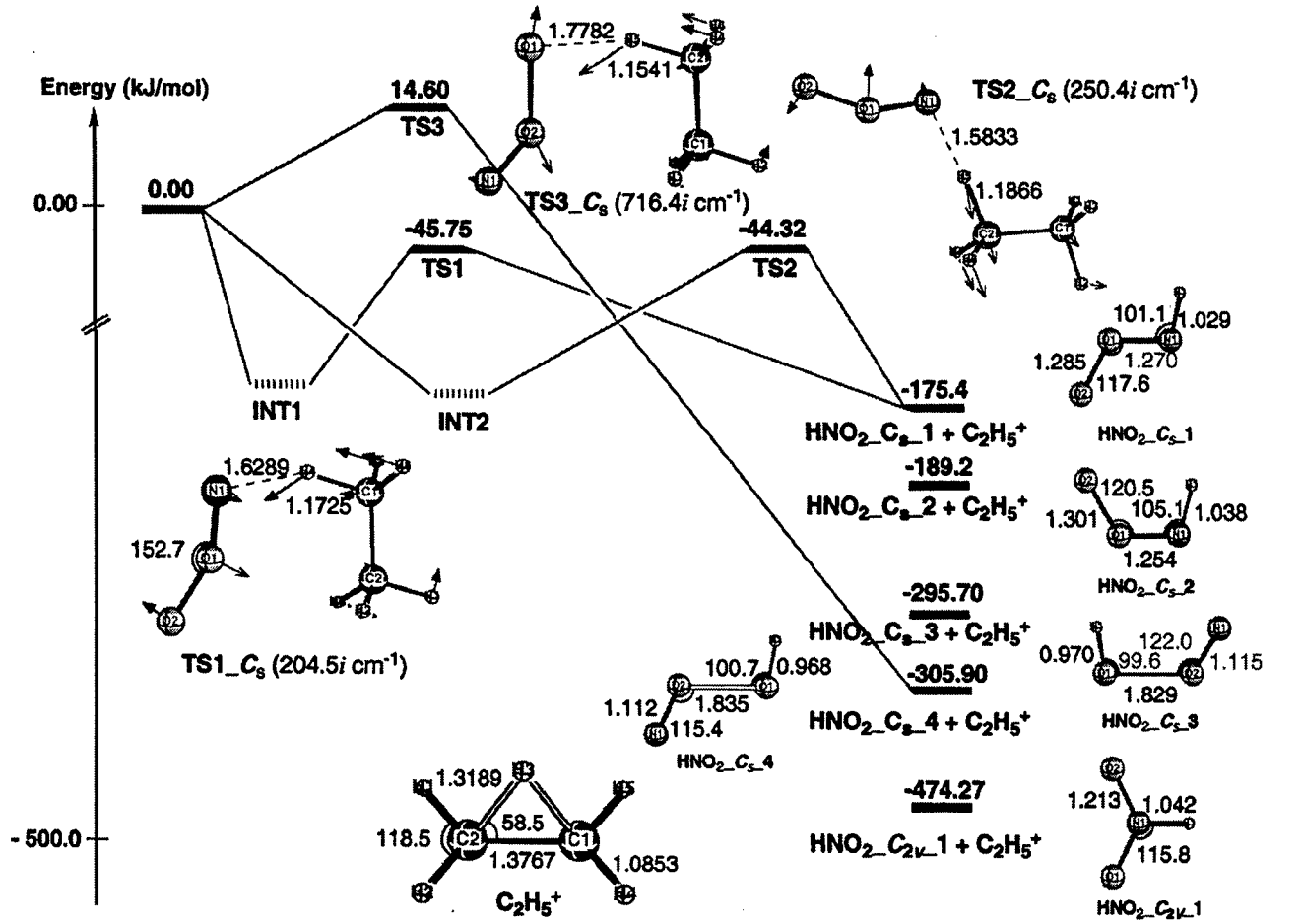

FIG. 5. ZPE corrected potential energy surface for the reaction of $NOO^+ + C_2H_6$. Numbers on the structures refer to the bond length (Å) and bond angles (degree). The vectors on the TS structures correspond to the reaction coordinates with their imaginary frequencies given in the parentheses. The product HNO_2 structures are labeled with the symmetry of the species in the name and are numbered from the highest energy product starting as number 1 to the lowest energy product of a given symmetry.

tion along the first two low energy pathways could proceed quite easily, which explains the nearly 100% efficiency of this reaction.

V. CONCLUSIONS

The NOO^+ ion was found to be highly reactive with most neutral molecules, except for some species with high ionization potentials. All neutral species with an IP ≤ 11.18 eV reacted with NOO^+, in part by charge transfer. Detailed calculations showed that the adiabatic and vertical IPs of NOO were about 10.4 and 11.7 eV, respectively. The observed experimental limit of 11.18 eV agreed well with the theoretical charge transfer energetics of the final products, assuming $X^+ + [O(^2P) + NO(^2\Pi)]$ formed via dissociation of metastable NOO during the reaction. The neutral reagent IP must thus be less than $(IP^{ad}(NOO) - \Delta E_{(O+NO)-NOO}) = \sim 11.1$ eV for the overall charge exchange reaction to be exothermic. This case would be dissociative charge transfer where the neutral product dissociated instead of the ionic product.

Formation of NO^+ product ions was also very common. In at least some of the reactions, this product ion might be due to collisions of NOO^+ with neutral X overcoming a dissociation barrier, especially since NOO^+ is separated from $NO^+ + O$ by a barrier of 0.88 eV.[6] Collision induced isomerization to the lowest energy ONO^+ isomer was also found in the reactions of NOO^+ with CS_2 and SO_2. Several of the reactions had numerous product channels. The CS_2 reaction, in particular, resulted in six different products.

ACKNOWLEDGMENTS

Two of the authors (A.A.V. and A.J.M.) would like to thank the Air Force Office of Scientific Research (AFOSR) for its continued support of this laboratory under Task No. 2303EP4. One of the authors (A.J.M.) was supported through Boston College Contract No. FA8718-04-C-0006. Another author (A.I.F.) was supported under the NRC Research Associate program. The work done at Emory University was supported in part by a grant from AFOSR (F49620-01-1-0183). Computer resources were provided in part by the Air Force Office of Scientific Research DURIP grant (FA9550-04-1-0321) as well as by the Cherry Emerson Center for Scientific Computation at Emory University and by a grant from AFOSR under the DoD High Performance Computing Program.

[1] D. B. Dunkin, F. C. Fehsenfeld, A. L. Schmeltekopf, and E. E. Ferguson, J. Chem. Phys. 54, 3817 (1971).
[2] D. Smith, N. G. Adams, and T. M. Miller, J. Chem. Phys. 69, 308 (1978).

[3] W. Lindinger, J. Chem. Phys. **64**, 3720 (1976).
[4] K. Hiraoka, J. Chem. Phys. **91**, 6071 (1989).
[5] S. Matsuoka, H. Nakamura, and T. Tamura, J. Chem. Phys. **75**, 681 (1981).
[6] S. Popovic, A. J. Midey, S. Williams, A. Fernandez, A. A. Viggiano, P. Zhang, and K. Morokuma, J. Chem. Phys. **121**, 9481 (2004).
[7] S. Matsuoka, H. Nakamura, and T. Tamura, J. Chem. Phys. **79**, 825 (1983).
[8] K. Hiraoka and S. Yamabe, J. Chem. Phys. **90**, 3268 (1989).
[9] A. A. Viggiano and R. A. Morris, J. Phys. Chem. **100**, 19227 (1996).
[10] A. A. Viggiano, R. A. Morris, F. Dale, J. F. Paulson, K. Giles, D. Smith, and T. Su, J. Chem. Phys. **93**, 1149 (1990).
[11] T. H. Dunning, Jr., J. Chem. Phys. **90**, 1007 (1989).
[12] P. Celani and H.-J. Werner, J. Chem. Phys. **112**, 5546 (2000).
[13] H.-J. Werner and P. J. Knowles, J. Chem. Phys. **82**, 5053 (1985).
[14] P. J. Knowles and H.-J. Werner, Chem. Phys. Lett. **115**, 259 (1985).
[15] P. J. Knowles, C. Hampel, and H.-J. Werner, J. Chem. Phys. **99**, 5219 (1993).
[16] J. D. Watts, J. Gauss, and R. J. Bartlett, J. Chem. Phys. **98**, 8718 (1993).
[17] P. J. Knowles and H.-J. Werner, Chem. Phys. Lett. **145**, 514 (1988).
[18] H.-J. Werner and P. J. Knowles, J. Chem. Phys. **89**, 5803 (1988).
[19] S. R. Langhoff and E. R. Davidson, Int. J. Quantum Chem. **8**, 61 (1974).
[20] H. J. Werner, P. J. Knowles, R. D. Amos, *et al.* MOLPRO, Version 2002.6, University of Birmingham, Birmingham, UK, 2002.
[21] P. J. Linstrom and W. G. Mallard, *NIST Chemistry WebBook* (National Institute of Standards and Technology, Gaithersburg, MD, 2003).
[22] M. J. Frisch, G. W. Trucks, H. B. Schlegel *et al.*, GAUSSIAN 03, Revision B.02, Gaussian, Inc., Pittsburgh, PA, 2003.
[23] L. Andrews, P. Hassanzadeh, G. D. Brabson, A. Citra, and M. Neurock, J. Phys. Chem. **100**, 8273 (1996).
[24] A. G. Baboul, L. A. Curtiss, P. C. Redfern, and K. Raghavachari, J. Chem. Phys. **110**, 7650 (1999).
[25] Y. Hayakawa, N. Terasawa, E. Hayashi, and T. Abe, Polymer **39**, 4151 (1998).
[26] H. Fukaya, E. Hayashi, Y. Hayakawa, and T. Abe, J. Fluorine Chem. **83**, 117 (1997).
[27] T. M. Sack, R. L. Lapp, M. L. Gross, and B. J. Kimble, Int. J. Mass Spectrom. Ion Process. **61**, 191 (1984).
[28] T. Su and W. J. Chesnavich, J. Chem. Phys. **76**, 5183 (1982).
[29] T. Su, J. Chem. Phys. **89**, 5355 (1988).
[30] T. J. Lee and P. R. Taylor, Int. J. Quantum Chem. **S23**, 199 (1989).
[31] P. Hassanzadeh and K. K. Irikura, J. Phys. Chem. A **101**, 1580 (1997).
[32] G. K. Jarvis, K. J. Boyle, C. A. Mayhew, and R. P. Tuckett, J. Phys. Chem. A **102**, 3230 (1998).